# CO J = 32 and J = 21 mapping and spectroscopy of NGC 7027

Astron. Astrophys. 151, 421–426 (1985)

ASTRONOMY AND ASTROPHYSICS

# CO $J=3\rightarrow2$ and $J=2\rightarrow1$ mapping and spectroscopy of NGC 7027

**J.P. Phillips, G.J. White, and K.J. Richardson**

Physics Department, Queen Mary College, Mile End Road, London E1 4NS, England

Received October 22, 1984; accepted April 25, 1985

**Summary.** We present spectra and mapping for NGC 7027 in the $J=2\rightarrow1$ and $J=3\rightarrow2$ transitions of CO. The central profile at $J=2\rightarrow1$ is shown to be very similar to the $J=1\rightarrow0$ spectrum measured by Thronson (1983), and this implies a source expansion at roughly constant velocity. The $J=3\rightarrow2$ line however appears weaker, with evidence for appreciable quenching of the higher velocity components. Detailed modelling of the source indicates that densities $n$ must vary appreciably with shell radius $R$ (as $n\propto R^{-\alpha}$, where $\alpha\geqq2$), and this leads to a corresponding steep radial decrease in the radiation temperature $T_R$. In consequence, the source FWHM is found to decrease appreciably with increasing transition frequency, a trend which appears also to be confirmed by our central $J=3\rightarrow2$ scans. It is not however possible to constrain gas kinetic temperatures $T_k$, the level of CO thermalisation, or shell mass $M_s$ with any degree of confidence – both low and high mass models appear capable of replicating our spectra.

Finally, the $J=2\rightarrow1$ spatial velocity map displays evidence for a decrease in velocity width towards the outer regions of the nebula; a feature which is expected of most outflow models. The $J=3\rightarrow2$ map also indicates the presence of a nebular extension to the north-west of the peak emission core, although this is not reproduced in the corresponding $J=1\rightarrow0$ map of Mufson et al. (1975).

**Key words:** NGC 7027 – CO spectroscopy – mapping

## 1. Introduction

NGC 7027 may perhaps lay claim to being the most heavily investigated of planetary nebulae, and has been observed and mapped over a greater range of wavelengths than any other comparable object. It remains, nonetheless, a distinctly uncharacteristic and anomalous representative of its class. The central star for instance has yet to be reliably identified, although perhaps the most persuasive case for detection suggests an unusually low visual luminosity, and a correspondingly high temperature $T_*>2\cdot10^5$ K (Atherton et al., 1979). The strength of $H_2$ $\lambda$ 2.1 μm quadrupole emission is also amongst the highest of any planetary so far detected (cf. Beckwith et al., 1980; Smith et al., 1981), as indeed are the near- and far-infrared dust emission excesses (cf. Moseley, 1980; Gillett et al., 1973; McCarthy et al., 1979), implying substantial masses of cool, neutral, and shocked gas. The appreciable local extinction ($A_V\sim1.5$ magnitudes; Atherton et al., 1979) appears to be associated with an enveloping neutral cloud of diameter $>0.75$ arcmin, and this has been measured and mapped in the $J=2\rightarrow1$ and $J=1\rightarrow0$ transitions of CO (Mufson et al., 1975; Knapp et al., 1982; Thronson, 1983), and in HCN (Olofsson et al., 1982). Apart indeed from various possible protoplanetary sources (such as CRL 618 and CRL 2688; Zuckerman et al., 1977; Lo and Bechis, 1976; Knapp et al., 1978), and a weak and uncertain detection for IC 418 (Mufson et al., 1975; Knapp et al., 1982), it remains the only well established planetary in which millimetre wave molecular lines have been definitively observed.

Estimates of the mass of this neutral gas range from $\sim0.4D^2M_\odot$ (based on early $J=1\rightarrow0$ CO mapping; Mufson et al., 1975), to $>5D^2M_\odot$ (determined from $J=2\rightarrow1$ narrow beam results; Knapp et al., 1982), and $\sim0.9D^2$ (from the $H_2$ quadrupole measures of Beckwith et al., 1980). The lowest and most recent estimate appears to be that of Thronson (1983), who used a high signal to noise $J=1\rightarrow0$ CO spectrum to determine $M_s\sim0.05D^2$, where $D$ is the distance in kiloparsecs. Given that $D$ is probably no less than $\sim1$ kpc (Pottasch et al., 1982), it is clear (from most of these estimates) that the neutral shell mass $M_s$ must be large, even allowing that the precise value of $M_s$ is uncertain. Such a conclusion would also be consistent with certain recent models of mass ejection in low to intermediate mass stars.

In the analysis of Renzini and Voli (1981), for instance, the shell C/O ratio is found to increase rapidly with progenitor mass, and exceeds unity for $M_*>2M_\odot$. Towards higher masses, however, it is found that CNO processing becomes important at the base of the convective envelope (the so-called hot-bottom burning), leading to the efficient conversion of $^{12}C$ into $^{14}N$. This appears sufficient to swamp $^{12}C$ enrichment in the third and final "dredge-up" phase, during which the convective envelope reaches past the H-He discontinuity. The shell composition, in consequence, again declines below C/O$\sim1$ for $M_*>5M_\odot$.

In general, therefore, it is probable that the large C/O ratio in NGC 7027 ($\sim3$: Shields, 1978; Perinotto et al., 1980; Pottasch, 1983) can be translated to imply a progenitor mass range $2<M_*/M_\odot<5$, and a corresponding shell mass of order $1\rightarrow2.5M_\odot$.

In the following, we attempt to further define the characteristics of the HI zone through spectroscopy and mapping in the $J=2\rightarrow1$ and (for the first time) $J=3\rightarrow2$ transitions of CO. The observations were acquired in November 1983 using the QMC submillimetre wave receiver mounted on the United Kingdom Infrared Telescope (UKIRT) in Hawaii. The corresponding instrumental beamsizes were measured to be 83 and 55 arcsec for the

*Send offprint requests to:* J.P. Phillips

$J=2\rightarrow1$ and $J=3\rightarrow2$ transitions respectively, the velocity resolution was 1.5 km s$^{-1}$, and system noise temperatures ranged from 180 K at 230 GHz to 350 K at 345 GHz.

The values for the forward spillover ($\eta_{fs}$) and coupling factor appropriate to a 45 arcsec diameter source ($\eta_c$) have been determined from measurements of Jupiter, Saturn, Venus and the Moon, and are 0.84 and 0.21 at 230 GHz, and 0.88 and 0.40 at 345 GHz respectively. The measured antenna temperatures derived from the usual chopper calibration, $T_A^*$, have been divided by $\eta_{fs}$ to obtain $T_R^*$, and further divided by $\eta_c$ to obtain an estimate of the brightness temperature $T_R$.

Sky opacities were typically excellent over the relevant observing term, with the 345 GHz transmittance at all times greater than 0.85 airmass$^{-1}$.

## 2. Observations

Central spectra for the $J=3\rightarrow2$ and $J=2\rightarrow1$ transitions of CO, together with a comparative $J=1\rightarrow0$ spectrum from Thronson (1983) are presented in Fig. 1. For direct comparison, these have been scaled to give appropriate brightness temperatures for an assumed (constant) source diameter of 45 arcsec (Knapp et al., 1982; Mufson et al., 1975; where we have employed the recent NRAO calibration of Kutner et al. (1984) for the spectrum of Thronson). As a result, it is seen that peak brightness temperatures in the $J=2\rightarrow1$ and $J=1\rightarrow0$ transitions appear broadly comparable, both to each other, and to the value of $T_R^*$ ($J=2\rightarrow1$) determined by Knapp et al. (1982) with narrow beam ($B=25$ arcsec) scans. Note, for reference, that peak antenna temperatures $T_R^*$ were measured to be 2.0 K and 2.2 K for the $J=2\rightarrow1$ and $J=3\rightarrow2$ lines respectively (where $T_R^*$ and $T_R$ represent the revised antenna and source radiation temperatures as defined by Kutner and Ulich, 1981).

The FWHM of the lower transition lines appear also to be broadly comparable, and suggest (with the flat-topped to parabolic profiles) a predominantly constant velocity gas outflow; a situation, in fact, which is reminiscent of certain other high mass-loss evolved objects (such as IRC 10216 and CIT 6), and which has been analysed in detail by Kuiper et al. (1976), Morris (1980), and others. The $J=3\rightarrow2$ spectrum by comparison appears to be substantially different in width, shape, and strength. The FWHM of the $J=3\rightarrow2$ line for instance is $\sim$13 km s$^{-1}$, roughly half that of the lower frequency transitions, and the value of $T_R$ is similarly down by a factor of one third (although the assumption of constant source size may be inapplicable – see later). With this in mind, therefore, we have been particularly careful in checking beam location on the source – a shift away from source centre by as little as $\sim$0.5 bandwidths, for instance, may cause an appreciable decrease in the apparent line width, as illustrated in Fig. 2 for $J=2\rightarrow1$. A comparison of the relevant peak antenna temperature with the maximum of our $J=3\rightarrow2$ map, however, shows that both are equal within errors.

The $J=2\rightarrow1$ spatial-velocity map in Fig. 2 appears to be barely resolved, and would be consistent with emission over a projected zone of diameter $\sim$1 arcmin or so. In particular, these scans show clear evidence for a narrowing of the lines at the source extremities – broadly as would be expected for most (spherically symmetric) outflow models. The $J=3\rightarrow2$ map in Fig. 3 also indicates a strong (and essentially unresolved) feature centred on the optical neblosity, with an appreciable emission spur extending towards the north-west – a characteristic which is not replicated in either the reflection nebula found by Atherton et

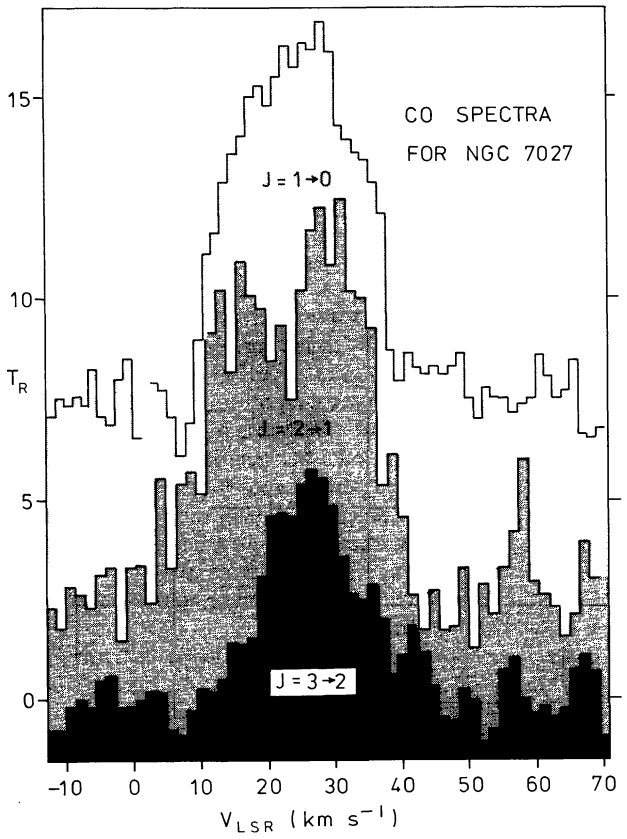


**Fig. 1.** Central spectra for NGC 7027 in the CO $J=3\rightarrow2$ (*lower profile*), $J=2\rightarrow1$, and $J=1\rightarrow0$ (*upper profile*) transitions. The temperature scale represents $T_R$, and corresponds to a source with diameter 0.75 arcmin. The $J=1\rightarrow0$ profile is by Thronson (1983), and has been scaled in accordance with the recent NRAO calibration of Kutner et al. (1984)

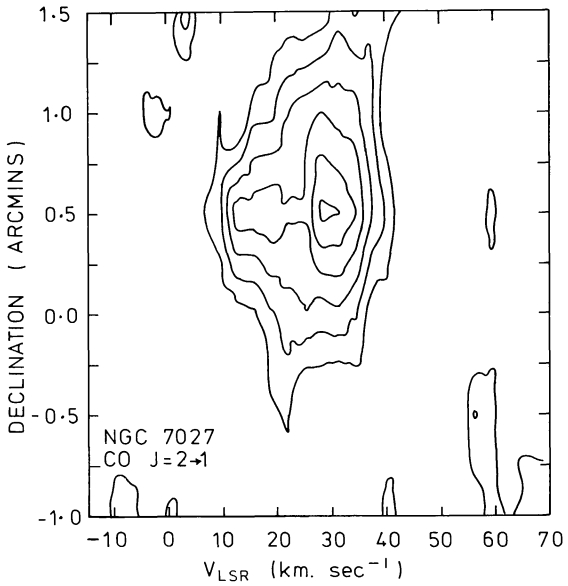


**Fig. 2.** Spatial-velocity map at CO $J=2\rightarrow1$. The lowest contour corresponds to $T_R^*=0.4$ K, with succeeding contours representing increments of 0.3 K. For this map, adjacent velocity channels have been merged to give an effective velocity resolution of 3.0 km s$^{-1}$

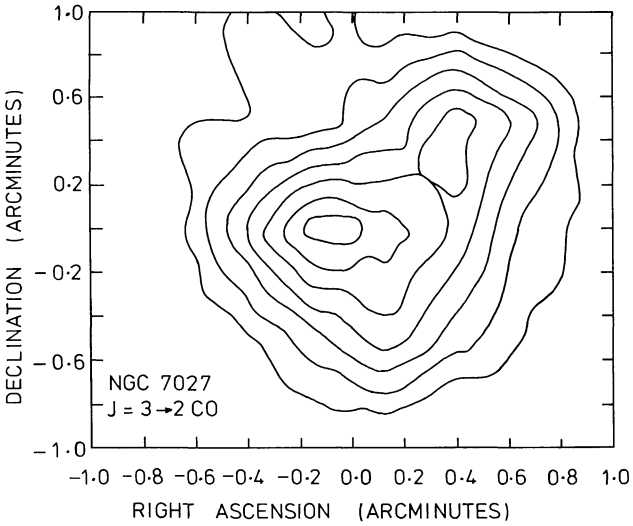


**Fig. 3.** $J=3\rightarrow 2$ CO map of NGC 7027 at $V_{LSR}=28\,\mathrm{km\,s^{-1}}$. The lowest contour represents $T_R^*=0.5\,\mathrm{K}$, whilst succeeding contours represent increments of 0.3 K

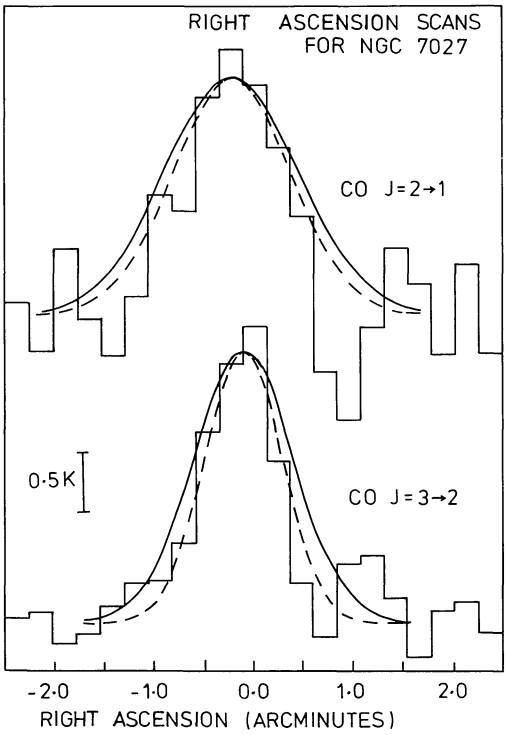


**Fig. 4.** Central scans for NGC 7027 in CO $J=2\rightarrow 1$ and $J=3\rightarrow 2$. Although the $J=2\rightarrow 1$ scan appears the broader, both profiles are in fact barely more extended than the expected point source response function (*dashed curves*). The convolution of our beams with a 45 arcsec FWHM gaussian source is indicated by the solid curve

al. (1979), or the $J=1\rightarrow 0$ map of Mufson et al. (1975). The compact nature of the core emission source is further illustrated in Fig. 4, where we compare central (sidereal rate) scans taken at $J=3\rightarrow 2$ and $J=2\rightarrow 1$. The different apparent widths of these profiles reflects the comparative beam sizes, and there is no evidence of the broadening to be expected for an appreciably extended source profile. Indeed, the scan at $J=3\rightarrow 2$ appears to suggest an emission zone which is extremely compact with respect to the beam, and certainly smaller than the mean FWHM $\sim 45$ arcsec appropriate to the lower frequency transitions.

## 3. Discussions

Previous analyses of the H I mass fraction in NGC 7027 have taken the lower rotational transitions of CO to be thermalised – an assumption which has profound implications for the adopted gas kinetic temperature $T_K$, and various other dependent parameters. Knapp et al. (1982) for instance were able to derive an $H_2$ excitation density $n(H_2)>10^4\,\mathrm{cm^{-3}}$, and a corresponding lower limit shell mass $M_s>5D^2\,M_\odot$ (for a source diameter $\sim 45$ arcsec) by assuming thermalisation of the $J=2\rightarrow 1$ transition. Mufson et al. (1975) were similarly able to deduce a $J=1\rightarrow 0$ mass of $\sim 0.4D^2M_\odot$ by deriving a column density $N(^{13}\mathrm{CO})$ $\sim 9.25\cdot 10^5\,\mathrm{cm^{-2}}$, and multiplying this by a value $\mathrm{H}/^{13}\mathrm{C}$ pertinent for I.S. clouds taken generally. Thronson (1983) however has noted that if O/H ratios appropriate to the ionised zone are adopted, then the derived column density of CO leads to a very different value for the shell mass of $\sim 0.05D^2M_\odot$ – an order of magnitude lower.

All of these mass estimates rely on a series of relatively insecure assumptions, and Thronson has noted that if clumping is large, then the value of $M_s$ due to Knapp et al. may be appreciably reduced. To bring this larger value of $M_s$ into agreement with the Thronson value, however, would require an extreme degree of clumping, and imply a volume filling factor $\varepsilon\sim 10^{-2}$. This in turn can be shown to imply a ratio $r_c/R_0<3/4\pi\varepsilon\sim 1/400$, where $r_c$ is a representative clump radius, and $R_0$ is the source radius. It is apparent therefore that unless the excitation temperature $T_{ex}(J=1\rightarrow 0)$ is significantly greater than $T_R(J=1\rightarrow 0)$, then the typical clump size must be extraordinarily small.

In the following, we shall model the source in terms of an heterogeneous outflow at constant velocity. We shall also assume a power-law density variation

$$n(\mathrm{H_2})=n_0\left(\frac{R_I}{R}\right)^{\alpha} \tag{1}$$

through the H I shell, where $R_I$ is the inner radius (corresponding to the H II zone radius $\sim 4.5$ arcsec), and the outer radius takes a value $R_0\gtrsim 5R_I$. To evaluate the temperature variation through this envelope, we note that where normal molecular line cooling dominates (Goldsmith and Langer, 1978) then

$$T_K\simeq T_{K_0}\left(\frac{R_I}{R}\right)^{-0.7\left(\frac{2}{\gamma+4}+0.1\,\alpha\right)} \tag{2}$$

$$(n(\mathrm{H_2})<0.1\,(X(\mathrm{CO})/dv/dz)^{-1})$$

where $T_K$ is the kinetic temperature, $X(\mathrm{CO})$ is the abundance of CO compared to $H_2$, $dv/dz$ is the line of sight velocity gradient (in $\mathrm{km\,s^{-1}pc^{-1}}$), and the relation assumes a grain emissivity law $\varepsilon\propto\lambda^{-\gamma}$. Expression (2) also applies strictly where the ratio $T_K/T_d$ is constant, or very much less than unity., where $T_d$ is the local dust temperature.

The relatively shallow variation represented by this expression derives from a balance between increased grain-gas coupling at higher densities, and an appreciable decrement in line cooling rates as the gas density decreases (Goldsmith and Langer, 1978).

Where the dust temperature takes a value $T_d \sim T_K$, however, then we anticipate $T_K \sim \propto R^{-2/(\gamma+4)}$.

These relations do not account for the contributions of fine structure line emission. Strong O I and C II emission in this source almost certainly arises predominantly at the H I/H II interface, either as a result of postshock cooling, direct UV excitation, or some similar mechanism (s) (Melnick et al., 1981; Crawford et al., 1985). FIR emission by C I will also be expected to contribute significantly, although the relevant transitions have yet to be detected in this source (cf. Beichman et al., 1983).

This latter cooling agent is of particular interest, both because of the large C/O ratio in NGC 7027, and the unexpected prevalence of C I at locations deep within molecular clouds (cf. Phillips and Keene, 1982; Phillips and Huggins, 1981). It would appear, therefore, that C I is an important coolant in both atomic and molecular H I zones, with kinematic and spatial distributions which are often similar to those for CO. This, in part, reflects the similar collisional and spontaneous emission rates for the two species (cf. Nussbaumer, 1971; Yau and Dalgarno, 1976), and it is probable that the volume emission trends are also not disimilar.

On balance, therefore, it is probable that the variation of $T_K(R)$ is shallow for any reasonable range of parameters $\alpha$, $\gamma$. Whilst the precise trend for kinetic temperature is uncertain, our final conclusions are comparatively insensitive to $T_K(R)$; any reasonably small gradient variation should lead to similar results. We will therefore employ expression (2) in the proceeding analysis.

Taking $\delta \cong 1$ and assuming an outflow velocity $v_{exp} = 14\,\mathrm{km\,s^{-1}}$, we have numerically solved the equations of radiative transfer for the lowest ten CO transitions, and a matrix of points in the $p-V_z$ plane (where $V_z$ represents the line of sight velocity, and $p$ is the impact parameter). CO–$H_2$ collisional rates were taken from Green and Thaddeus (1976), and have been appropriately weighted for the contribution of He. Transitions up to $J=3$ were then convolved with the appropriate instrumental beam profiles, to yield comparative model values for $T_R^*$. Whilst the LVG formalism employed here is not strictly applicable for constant velocity flows (where the Sobolev approximation breaks down), the deviations from strict LVG requirements are relatively unimportant. The line-of-sight velocity gradient through the shell is large, for instance, and results in an extremely small self-absorption solid-angle. The interaction between different regions of the envelope is, therefore, comparatively small.

Representative examples of our modelling are illustrated in Fig. 5, where we have adopted an outer shell radius $R_0 = 0.22\,\mathrm{pc}$ (corresponding to an angular diameter $\theta_0 \sim 1.5\,\mathrm{arcmin}$ at $D = 1\,\mathrm{kpc}$; twice the FWHM estimated from observations at $J=1\rightarrow 0$ and $J=2\rightarrow 1$). Appreciably smaller values of $R_0$ led to line intensity ratios which were at variance with our observations. Larger values on the other hand could not be discounted, although they made little difference to our final spectra.

The results, as can be seen, are in reasonable agreement with the observed lower frequency transitions. In particular, line intensities are reproduced tolerably well, and the line profiles show the characteristic steep-sided signature relevant to this and many other late-type sources. Most important, however, is the fact that both *high and low temperature models are capable of replicating the profiles,* at least insofar as the lower frequency transitions are concerned. The CO lines are therefore not necessarily thermalised throughout the source envelope.

We should perhaps add, at this point in the discussion, that the analysis above does not allow for various other possible constraints. The extinction arising from the shell appears to be of order $A_v \sim 1.5\,\mathrm{mag}$, for instance, and this can be shown

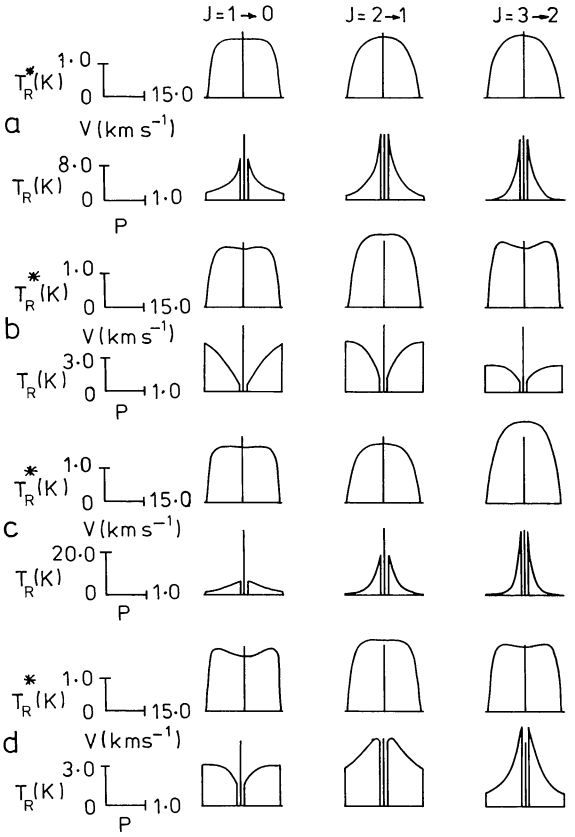


**Fig. 5.** Model profiles and ($V = 0\,\mathrm{km\,s^{-1}}$) shell emission structures for constant velocity outflows, where $p$ is the impact parameter in units of $R_0$, $V$ is gas velocity with respect to the LSR, and $T_R^*$ and $T_R$ are the antenna and radiation temperatures. The models have been convolved with relevant UKIRT ($J=2\rightarrow 1$, $J=3\rightarrow 2$) and NRAO ($J=1\rightarrow 0$) beam profiles. Note that the NRAO beam parameters are taken to be those in force prior to recent upgrading of the 11 metre telescope, and refer to measurements taken before the summer of 1982. The models parameters are as follows:
(a) $T_0 = 22\,\mathrm{K}$, $n_0 = 4.3\,10^5\,\mathrm{cm^{-3}}$, $\alpha = 2$, $X(\mathrm{CO}) = 10^5$;
(b) $T_0 = 20\,\mathrm{K}$, $n_0 = 6.0\,10^4\,\mathrm{cm^{-3}}$, $\alpha = 0$, $X(\mathrm{CO}) = 2.1\,10^{-6}$;
(c) $T_0 = 78\,\mathrm{K}$, $n_0 = 5.0\,10^4\,\mathrm{cm^{-3}}$, $\alpha = 2$, $X(\mathrm{CO}) = 1.2\,10^{-4}$;
(d) $T_0 = 54\,\mathrm{K}$, $n_0 = 3.8\,10^4$, $\alpha = 1$, $X(\mathrm{CO}) = 2.9\,10^{-5}$

to imply a mass $\sim 1.4\,M_\odot$ for an assumed "normal" ratio $A_v/N(\mathrm{H_2}) \sim 10^{-21}\,\mathrm{mag}$ – a result which is relatively independant of the degree of clumping. Similarly, if molecular line cooling dominates in the H I shell (and its contribution can hardly be less than significant), then we determine a CO abundance

$$X(\mathrm{CO}) \simeq \frac{4.10^{-8} T_d}{(T_K/10)^{1.4}} \left[\frac{n(\mathrm{H_2})}{10^3}\right]^{0.1} \left[\frac{a}{0.1\,\mu\mathrm{m}}\right]^{-1} \left[\frac{\chi}{10^{-2}}\right] \qquad (3)$$

from Goldsmith and Langer (1978) and Leung (1975), where $\chi$ is the dust to gas mass ratio. Taking a dust temperature $T_d \cong 90\,\mathrm{K}$ based on IRAS and other results (cf. Moseley, 1980; Pottasch, 1983), $n(\mathrm{H_2}) \cong 2.5 \cdot 10^4\,\mathrm{cm^{-3}}$, a mean grain size $a \cong 0.05\,\mu\mathrm{m}$, and $\chi \simeq 10^{-2}$ (Natta and Panagia, 1981) then gives $T_K^{1.4}$ $X(\mathrm{CO}) \sim 2.5 \cdot 10^{-4}$. Mapping this onto the range of viable LVG solutions (in the $X(\mathrm{CO})/dv/dz - n(\mathrm{H_2})$ plane) then indicates the necessity for large $H_2$ densities ($n(\mathrm{H_2}) > 10^4\,\mathrm{cm^{-3}}$), and a substantial level of shell thermalisation.

Arguably, therefore, the shell is more likely to be thermalised (and of high density) than otherwise. Nevertheless, the present

analysis illustrates that estimates of mass based on the CO lines alone are by no means as secure as previously assumed. In particular, the convenience of a *constant density* thermalised shell (utilised in previous mass estimates) is revealed as quite inadaquate. When the possible effects of clumping are introduced, then of course the level of uncertainty becomes even larger.

For purposes of comparison, we may note that the masses of our illustrated models range between $M_s/M_\odot \sim 130\,\varepsilon$ for 5b, through to $\sim 25\,\varepsilon$ for 5a, and finally $\sim 3\,\varepsilon$ in the case of 5c. All of our models therefore have large values of $M_s/\varepsilon$, although lower masses appear also to be plausible. For certain cases, therefore, it is plain that either the progenitor mass is required to be (unrealistically) high, or the volume filling factor $\varepsilon$ extremely small – a condition which of itself would not be unreasonable, given the observed patchy extinction in this source.

The value of $\alpha$, the density radial exponent, appears to be a little easier to constrain. All of the models resulting in viable profiles suggest an unsatisfactory $J=1\rightarrow 0$ source structure where $\alpha \leqq 1$, with the source brightness temperature $T_R$ declining as the projected radius decreases. This is not however the case where $\alpha \leqq 2$, and it appears likely that the density gradient is, therefore, relatively steep; in at least qualitative agreement with the trend for *grain* number density adduced by Atherton et al. (1979). We also find quite generally that the $J=3\rightarrow 2$ source width is less than for the lower frequency transitions, which would again be in agreement with the results presented here.

It is apparent, therefore, that an outflow envelope with small evacuated core can represent the observed line intensities reasonably well. It has also been found possible to reproduce the general trends in ($J=2\rightarrow 1$ and $J=1\rightarrow 0$) line shapes. The $J=3\rightarrow 2$ profiles, however, are less easy to comprehend. No constant velocity outflow of the kind outlined here could possibly reproduce the profile in Fig. 1; unless of course more than one mass component is present.

Perhaps the $J=3\rightarrow 2$ line is weighted by emission from denser regions of the nebular halo, close to the H II zone, which shock heating and compression also play a role. Alternatively, the flow characteristics for the inner zone may simply be less homogeneous and symmetric than for the greater part of the outflow volume, which is sampled by the proportionately larger beams at $J=2\rightarrow 1$ and $J=1\rightarrow 0$. On the present evidence, it is simply not possible to choose between these and other options.

Clearly, therefore, further observations at these and higher frequencies would be welcome, both to confirm the present $J=3\rightarrow 2$ spectrum, and to outline the area of $J=3\rightarrow 2$ emission. More specifically, the present modelling also illustrates the utility of higher resolution mapping (as a means of discriminating between various source models), and observations with larger antennas would therefore be of particular interest.

## 4. Conclusions

We have mapped the planetary nebula NGC 7027 in the $J=3\rightarrow 2$ and $J=2\rightarrow 1$ transitions of CO. The spectral profile at $J=2\rightarrow 1$ appears closely similar to that measured previously at $J=1\rightarrow 0$, and suggests a possible constant velocity outflow. The $J=3\rightarrow 2$ line however is radically different, with an appreciably different width and shape.

The reasons for this disparity in profiles are not clear, although the possibility of a multi-component and more complex shell cannot be discounted. In this respect, the evidence of irregular extinction across the source is of particular interest, suggesting as it does a rather uneven H I mass distribution. Observations at higher resolution (and frequency) should be of particular aid in resolving this question.

Detailed modelling of the profiles has been attempted using power-law expressions for the radial density and temperature variations. The temperature variation is assumed to be shallow, although the final results are not, otherwise, particularly sensitive to the radial exponent. The results of such an analysis are found to be in reasonable accord with observed antenna temperatures, and the line shapes at $J=1\rightarrow 0$ and $J=2\rightarrow 1$. It is apparent however that density gradients through the shell must be appreciable, with the radial density exponent $\alpha \geqq 2$. Similarly, the source FWHM is required to decrease significantly with increasing transition frequency $\nu_{J\rightarrow J-1}$; a trend apparently supported by our $J=3\rightarrow 2$ scans.

Neither the gas kinetic temperature $T_K$, nor the derivative shell mass $M_s$ are capable of being appreciably constrained through this modelling, and the CO line results above do not enable us to define the state of thermalisation. In consequence, previous estimates of shell mass can be regarded only as speculative estimates. It is nevertheless noted that a reasonably large shell mass may be required to explain the high levels of local extinction.

Finally, we have also mapped the source in the spatial-velocity plane at $J=2\rightarrow 1$, and demonstrate that although the nebula is barely resolved, the linewidth decreases significantly away from source centre. A $J=3\rightarrow 2$ spatial map at $V_{LSR}=28\,\mathrm{km\,s^{-1}}$ also suggests the presence of a nebular spur towards the northwest of the central source – an extension which is not however evident in the $J=1\rightarrow 0$ map of Mufson et al. (1975).

*Acknowledgements.* We would like to thank Dr. Lorne Avery for help with certain of the observations. We are also grateful to PATT for financial support towards travel and subsistence; to the staff of UKIRT for night assisting and support of the telescope, and their usual inestimable help in many other ways; and to the SERC for their support of the millimetre/submillimetre astronomy program at Qmc.

## References

Atherton, P.D., Hicks, T.R., Reay, N.K., Robinson, G.J., Worswick, S.P., Phillips, J.P.: 1979, *Astrophys. J.* **232,** 786
Beckwith, S., Neugebauer, G., Becklin, E., Matthews, K.: 1980, *Astron. J.* **85,** 886
Beichman, C.A., Keene, J., Phillips, T.G., Huggins, P.J., Wootten, H.A., Manson, C., Frerking, M.A.: 1983, *Astrophys. J.* **273,** 633
Crawford, M.K., Genzel, R., Townes, C.H., Watson, D.M.: 1985, *Astrophys. J.* (in press)
Gillett, F.C., Forrest, W.J., Merrill, K.M.: 1973, *Astrophys. J.* **183,** 87
Goldreich, P., Kwan, J.: 1974, *Astrophys. J.* **189,** 441
Goldsmith, P.F., Langer, W.D.: 1978, *Astrophys. J.* **222,** 881
Green, S., Thaddeus, P.: 1976, *Astrophys. J.* **205,** 766
Knapp, G.R., Phillips, T.G., Leighton, R.B., Lo, K.Y., Wannier, P.G., Wootten, H.A., Huggins, P.J.: 1982, *Astrophys. J.* **252,** 616
Kuiper, T.B.H., Knapp, G.R., Knapp, S.L., Brown, R.L.: 1975, *Astrophys. J.* **204,** 408
Kutner, M.L., Mundy, L., Howard, R.J.: 1984, *Astrophys. J.* (in press)
Kutner, M.L., Ulich, B.C.: 1981, *Astrophys. J.* **250,** 341

Leung, C.M.: 1975, *Astrophys. J.* **199,** 340
Lo, K.Y., Bechis, K.P.: 1976, *Astrophys. J.* **205,** L21
McCarthy, J.F., Forrest, W.J., Houck, J.R.: 1978, *Astrophys. J.* **224,** 109
Melnick, G., Russell, R.W., Gull, G.E., Harwit, M.: 1981, *Astrophys. J.* **243,** 170
Morris, M.: 1980, *Astrophys. J.* **236,** 823
Moseley, H.: 1980, *Astrophys. J.* **238,** 892
Mufson, S.L., Lyon, J., Marionni, P.A.: 1975, *Astrophys. J.* **201,** L85
Natta, A., Panagia, N.: 1981, *Astrophys. J.* **248,** 189
Nussbaumer, H.: 1971, *Astrophys. J.* **166,** 411
Olofsson, H., Johansson, L., Rien, N.Q., Sobka, R.J., Zuckerman, B.: 1982, *Bull. Amer. Astron. Soc.* **14,** No. 4
Perinotto, M., Panagia, N., Benvenuti, P.: 1980, *Astron. Astrophys.* **85,** 332
Phillips, J.P., Pottasch, S.R.: 1984, *Astron. Astrophys.* **130,** 91
Phillips, T.G., Huggins, P.J.: 1981, *Astrophys. J.* **251,** 533
Phillips, T.G., Keene, J.: 1982, In: The Scientific Importance of Submillimetre Observations, ESA SP-189
Pottasch, S.R.: 1980, *Astron. Astrophys.* **89,** 336
Pottasch, S.R.: 1983, *Planetary Nebulae,* D. Reidel Publishing Co., Dordrecht, The Netherlands
Pottasch, S.R., Gos, W.M., Arnal, E.M., Gauthier, R.: 1982, *Astron. Astrophys.* **106,** 229
Renzini, A., Voli, M.: 1981, *Astron. Astrophys.* **94,** 175
Robinson, G.J., Reay, N.K., Atherton, P.D.: 1982, *Monthly Notices Roy. Astron. Soc.* **199,** 649
Shields, G.A.: 1978, *Astrophys. J.* **219,** 565
Smith, H.A., Larson, H.P., Fink, U.: 1981, *Astrophys. J.* **244,** 835
Thronson, H.A.: 1983, *Astrophys. J.* **264,** 599
Yau, A.W., Dalgarno, A.: 1976, *Astrophys. J.* **206,** 652
Zuckerman, B., Palmer, P., Morris, M., Turner, B.E., Gilra, D.P., Bowers, P.F., Gilmore, W.S.: 1977, *Astrophys. J.* **211,** L79